Atmospheric Environment 343 (2025) 120982

Contents lists available at ScienceDirect

Atmospheric Environment

journal homepage: www.elsevier.com/locate/atmosenv

Investigation of priority anthropogenic VOCs in the large industrial city of Ulsan, South Korea, focusing on their levels, risks, and secondary formation potential

Seong-Joon Kim [a,b], Sang-Jin Lee [a,b], Youwei Hong [c], Sung-Deuk Choi [a,b,*]

[a] Department of Civil, Urban, Earth, and Environmental Engineering, Ulsan National Institute of Science and Technology (UNIST), Ulsan, 44919, Republic of Korea
[b] Research and Management Center for Particulate Matter in the Southeast Region of Korea, Ulsan National Institute of Science and Technology (UNIST), Ulsan, 44919, Republic of Korea
[c] Key Lab of Urban Environment and Health, Institute of Urban Environment, Chinese Academy of Sciences, Xiamen, 361021, China

HIGHLIGHTS

- Passive air samplers were used to monitor 59 VOCs at 21 sites in an industrial city.
- Toluene, ethylbenzene, and m,p,o-xylenes accounted for 56.9% of the total VOCs.
- Elevated concentrations of total VOCs were observed at most industrial sites.
- Toluene/benzene ratios indicated the dominance of fuel evaporation and solvent use.
- Aromatic compounds were frequently found on priority lists of the top 10 VOCs.

GRAPHICAL ABSTRACT

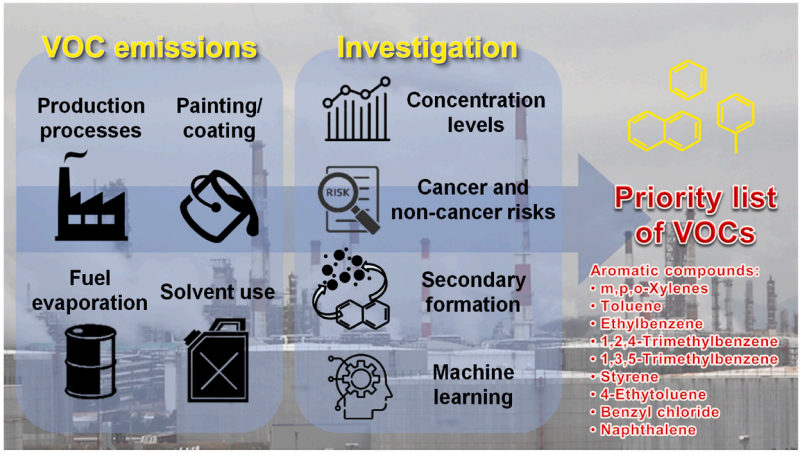

ARTICLE INFO

Keywords:
GIS
HAPs
Source identification
Risk
Machine learning

ABSTRACT

Volatile organic compounds (VOCs) are a concern due to their human health risks and secondary reactions, which vary according to the physicochemical properties and photochemical reactivity of individual VOCs. In this study, 59 VOCs were monitored using passive air samplers at 5 industrial and 16 urban sites in Ulsan, the largest industrial city in South Korea, over the course of a week (July 28–August 4, 2021). During the sampling period, toluene (4.6 μg/m^3), ethylbenzene (3.2 μg/m^3), and m,p,o-xylenes (8.5 μg/m^3) accounted for 56.9% of the total (Σ_{59}) VOCs. Elevated concentrations of Σ_{59} VOCs were observed in the automobile and shipbuilding industrial complexes, as well as at urban sites near the industrial complexes, due to dominant southeasterly winds. Toluene/benzene ratios indicated that fuel evaporation and solvent use were dominant during this warm

* Corresponding author. Department of Civil, Urban, Earth, and Environmental Engineering, Ulsan National Institute of Science and Technology (UNIST), Ulsan, 44919, Republic of Korea.
E-mail address: sdchoi@unist.ac.kr (S.-D. Choi).

https://doi.org/10.1016/j.atmosenv.2024.120982
Received 30 April 2024; Received in revised form 28 November 2024; Accepted 7 December 2024
Available online 7 December 2024

sampling period. Benzene and naphthalene exhibited the highest mean cancer and non-cancer risks, respectively; however, none of the risks exceeded the US EPA's tolerable and acceptable safety levels. Furthermore, secondary organic aerosol formation potentials (SOAFPs) of VOCs were estimated, with toluene contributing the most. Additionally, explainable artificial intelligence analysis suggested that styrene was closely related to $PM_{2.5}$ formation. Finally, priority lists of the top 10 VOCs based on their concentrations, risks, and SOAFPs were created, and aromatic compounds were frequently found on the lists. Based on these findings, customized management strategies for VOC reduction are recommended in multi-industrial cities.

1. Introduction

Atmospheric volatile organic compounds (VOCs) are emitted from various biogenic and anthropogenic sources, such as vehicular exhaust, industrial facilities, paints, and vegetation (Duan et al., 2023; Gu et al., 2021). These VOCs adversely impact air quality and human health. Over the last decade, atmospheric VOCs have become a major global concern due to their inhalation toxicity and potential for secondary reactions (Liu et al., 2023; Wang et al., 2023a).

Several VOCs, specifically benzene, toluene, ethylbenzene, and xylenes (BTEX), are classified as hazardous air pollutants (HAPs) by the United States Environmental Protection Agency (US EPA) (https://www.epa.gov/haps). Prolonged exposure to HAPs can lead to serious health problems (Rostami et al., 2021). For example, benzene is a hematotoxic chemical that can cause myeloid leukemia and aplastic anemia, and it poses risks to the lymphatic, central nervous, and blood-forming systems (Dehghani et al., 2019; Rostami et al., 2021). Toluene, ethylbenzene, and xylenes are neurotoxic and associated with brain disorders, eye irritation, skin inflammation, premature delivery, and respiratory, liver, and kidney problems (Mohammadi et al., 2020; Rostami et al., 2021). The risk levels and types of related diseases vary depending on the specific VOCs.

Furthermore, as VOCs are important precursors to secondary organic aerosol (SOA), their photochemical oxidation in the atmosphere significantly contributes to the formation of SOA, a major component of particulate matter (PM) (Zhan et al., 2021; Zhang et al., 2021). The photochemical reactivity and atmospheric lifetime of individual VOCs vary based on their physicochemical properties (Li et al., 2020a). Therefore, it is crucial to prioritize individual VOCs based on their human health risks and their potential for contributing to secondary reactions in the atmosphere.

In order to estimate the secondary organic aerosol formation potential (SOAFP), several methods have been developed, including the use of the fractional aerosol coefficient (FAC) (Grosjean, 1989), secondary organic aerosol potential (SOAP) (Derwent et al., 2010), and SOA Yield (Pandis et al., 1992). These approaches, which are based on VOC measurements (or emissions), chamber experiments, and modeling simulations, have been widely applied in ambient VOC studies across urban and industrial areas. For instance, hourly, daily, or weekly VOC measurement data have been used to calculate SOAFPs in various countries, such as Canada (Xiong et al., 2020), India (Kalbande et al., 2022), South Korea (Kim et al., 2022), Taiwan (Chen et al., 2023), and China (Wang et al., 2023b). These studies reported that aromatic compounds play a crucial role in secondary formations. However, research on spatial variations in SOAFPs using high-spatial-resolution data remains limited despite the availability of high-time-resolution data from previous studies.

The multi-industrial city of Ulsan, located on the southeast coast of the Korean Peninsula, has been concerned with air pollutants emitted from four industrial complexes: petrochemical, automobile, non-ferrous, and shipbuilding (Kim et al., 2019, 2023). According to the Pollutant Release and Transfer Registers (PRTR) system (https://icis.me.go.kr/prtr) in 2021, Ulsan exhibited the largest air emissions (7.0 tonne/km^2/y) of total toxic chemicals, including BTEX from industrial facilities in South Korea. Several monitoring campaigns conducted by the National Institute of Environmental Research (NIER) of Korea have reported on the concentration levels and risks of HAPs, including VOCs in Ulsan (NIER, 2010, 2020; 2021a). In our previous studies, the spatial distributions and major sources of VOCs in Ulsan were identified (Kim et al., 2019, 2023). However, these studies did not specifically address the secondary reactions of VOCs related to $PM_{2.5}$ formation in the atmosphere. Recently, from May 2020 to October 2022, the NIER conducted additional VOC monitoring campaigns (NIER, 2021b, 2022a, b, c), with some results now published (Lee et al., 2023, 2024a), which calculate the SOAFPs and sensitivity coefficients to better understand the relationship between VOCs and $PM_{2.5}$. Although previous studies have explored the secondary formation potential of VOCs at multiple sites in Ulsan, a comprehensive interpretation based on concentration levels, risks, and secondary formation is still required to efficiently manage VOC emissions.

In this study, passive air samplers (PASs) were deployed at 21 sites in Ulsan to analyze 59 VOCs, aiming to determine their concentration levels, spatial distribution, major sources, associated risks, and secondary reactions related to $PM_{2.5}$ formation. Additionally, explainable artificial intelligence (XAI) was applied to identify the priority VOC contributors to predicted ambient $PM_{2.5}$ levels. The ultimate goal of this research is to develop priority lists of VOCs. Given that the concentration levels, risks, and SOAFPs of VOCs vary depending on their physicochemical properties and the locations of the sampling sites, these priority lists based on high-spatial-resolution data can be useful for effectively managing VOC emissions from large industrial complexes in Ulsan.

2. Materials and methods

2.1. Sample collection and instrumental analysis

Duplicate PASs (Radiello®, Sigma-Aldrich, USA) were deployed at 5 industrial and 16 urban sites during a week (July 28–August 4, 2021) in Ulsan, South Korea (Fig. 1). The samplers at all sites were installed at heights between 2 m and 15 m above the ground. Air sampling was conducted as quickly as possible to minimize time differences, taking approximately 6 h to move from the first to the last site during both deployment on July 28 and collection on August 4. Sampling followed the same site order, with the driving route taken into consideration.

Each sampler consists of a yellow diffusive body (RAD 120-2) and an adsorbing cartridge (RAD 145) filled with graphitized charcoal (Carbograph 4, 530 ± 30 mg, 35–50 mesh). The cartridges were stored at −4 °C before and after sampling. After sampling, the collected cartridges were analyzed using a thermal desorption (TD) instrument (TD-100, Markes, UK) coupled with a gas chromatograph/mass spectrometer (GC/MS) (7890B/5977A, Agilent, USA). Detailed information on the procedures and conditions of instrumental analysis is presented in Text S1 in the Supplementary Information. For quality assurance/quality control (QA/QC), five-point calibration curves for the 59 target VOCs exhibited high coefficients of determination ($r^2 > 0.99$). Details of the calibration curves are presented in Table S1 in the Supplementary Information. Field blank samples were analyzed, showing concentrations ranging from 0.01 to 1.55 μg/m^3 for the 59 VOCs, and the final concentrations of individual species were blank-corrected. Additionally, the method detection limits (MDLs) for the 59 VOCs were determined using Eq (1) (Kim et al., 2019, 2021).

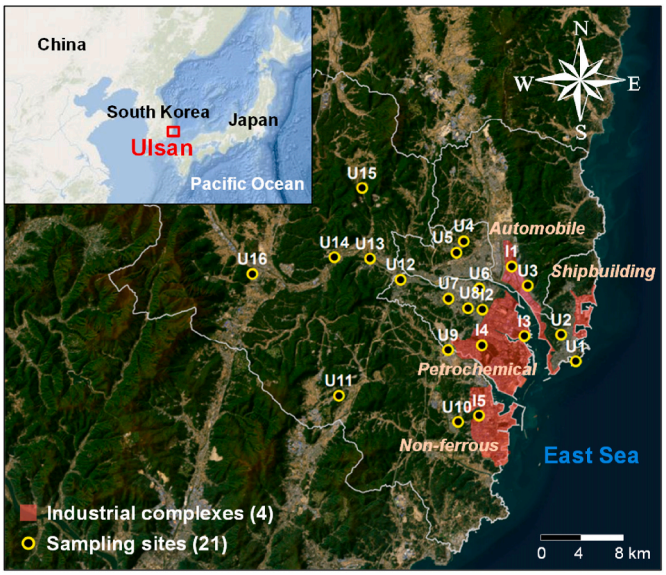

Fig. 1. Locations of 5 industrial and 16 urban sites for passive air sampling in Ulsan, South Korea. Four types of industrial areas along the East Sea are highlighted in red.

$$MDL = t_s \times SD \quad (1)$$

where t_s (3.14) is the Student's *t* value at the 99% confidence level (one-sided), and SD is the standard deviation of the concentration of seven replicate samples (0.05 μg/m^3) for individual VOCs. The MDLs are presented in Tables S2, and a further description of the calculation of air concentrations is provided in Text S2.

2.2. Meteorological conditions

Hourly meteorological data for 2021, including temperature, precipitation, relative humidity, wind speed, and wind direction, were obtained from a meteorological observatory (MO) located within 1 km of site U4 as well as from eight automatic weather stations (AWSs) (Fig. S1 in the Supplementary Information) operated by the Korea Meteorological Administration (https://data.kma.go.kr). The meteorological parameters for the four seasons of 2021 and the study period (July 28–August 4, 2021) at the MO in Ulsan are summarized in Table S3. An average wind field during the study period was modeled using the CALMET model (CALPUFF View version 9.0, Lakes Environmental, Canada), with detailed information provided in Text S3. Typically, northwesterly winds prevail in the study area, but during the study period, winds predominantly originated from the southeastern areas near industrial complexes along the East Sea, suggesting that air pollution could be enhanced in urban areas due to the southeasterly winds (Kim et al., 2019).

In addition, three-day backward air trajectories were generated using the HYSPLIT 5 model developed by the National Oceanic and Atmospheric Administration (NOAA) (https://www.ready.noaa.gov/HYSPLIT.php). The trajectories, arriving at the MO with starting heights at half of the planetary boundary layer (PBL) height, were calculated every 6 h during the sampling period. The trajectories were then depicted using TrajStat software (version 1.2.3.6).

2.3. Secondary organic aerosol formation potential

SOAFPs for individual VOCs can be calculated using three different methods: the FAC (Li et al., 2022), SOAP (Li et al., 2020a), and SOA Yield methods (Ait-Helal et al., 2014). Out of the 59 VOCs in this study, the calculation of SOAFPs was available for 10, 18, and 10 VOCs using the FAC, SOAP, and SOA Yield methods, respectively, as described in Eqs (2)–(4).

$$SOAFP_i = C_i \times FAC_i \quad (2)$$

$$SOAFP_i = \frac{C_i \times SOAP_i}{100} \times FAC_{toluene} \quad (3)$$

$$SOAFP_i = C_i \times Y_i \quad (4)$$

where $SOAFP_i$ represents the secondary organic aerosol formation potential of VOC *i* (μg/m^3), C_i is the concentration of VOC *i* (μg/m^3) in this study, FAC_i is the fractional aerosol coefficient of VOC *i* (%) (Grosjean, 1989, 1992), $SOAP_i$ is the secondary organic aerosol potential of VOC *i* (unitless) (Derwent et al., 2010), $FAC_{toluene}$ is the FAC of toluene (5.4%) (Grosjean, 1992), and Y_i is the SOA Yield of VOC *i* (μg/m^3/ppm) (Ng et al., 2007; Pandis et al., 1992). The values for individual VOCs used in these calculations are summarized in Table S2.

2.4. Risk assessment

Of the 59 target compounds, 13 and 26 VOCs are classified as carcinogens and non-carcinogens, respectively, according to the Integrated Risk Information System (IRIS) of the US EPA (https://iris.epa.gov/) and the International Agency for Research on Cancer (IARC) of the World Health Organization (WHO) (https://www.iarc.who.int/). In this study, a risk assessment was conducted using a deterministic risk assessment approach, which is widely used in previous studies (Baek et al., 2020; Kumar et al., 2018; Wu et al., 2011). Cancer and non-cancer risks were calculated using Eqs (5) and (6), respectively (US EPA, 2009).

$$Risk_i = C_i \times IUR_i \quad (5)$$

$$HQ_i = C_i \ / \ (RfC_i \times 1000\ \mu g / mg) \quad (6)$$

where $Risk_i$ represents the cancer risk for VOC *i*, C_i is the mean concentration (μg/m^3) of VOC *i* measured in this study, IUR_i means the inhalation unit risk for VOC *i* (μg/m^3)$^{-1}$, HQ_i denotes the hazard quotient for VOC *i*, and RfC_i is the reference concentration for inhalation exposure (mg/m^3) of VOC *i*. Ambient concentrations, rather than exposure concentrations, were used to examine the relative risk levels of specific VOCs emitted from the industrial complexes in Ulsan. The IURs for the 13 carcinogens and the RfCs for the 26 non-carcinogens are referenced from the IRIS, the California Office of Environmental Health Hazard Assessment (OEHHA), and the Agency for Toxic Substances and Disease Registry (ATSDR). These values are summarized in Table S2.

2.5. Explainable artificial intelligence (XAI)

The SHapley Additive exPlanations (SHAP) approach, an explanatory machine learning method, is widely used to determine the importance of input variables on output variables, such as concentrations of air pollutants (Hou et al., 2022; Stirnberg et al., 2021). Originating from game theory, SHAP quantifies the contribution of each player or variable in a predictive model (Lundberg and Lee, 2017). For each prediction, the Shapley value is calculated by assessing the change in the predicted value with and without a particular variable *i*. Each case is weighted, and the final Shapley value for variable *i* is calculated using Eq (7).

$$\varphi_i = \sum_{S \in F \setminus \{i\}} \frac{|S|!(|F|-|S|-1)!}{|F|} \left[f_{S\cup\{i\}}(x_{S\cup\{i\}}) - f_S(x_S) \right] \quad (7)$$

where φ_i represents the Shapley value for variable *i*, F is the set of all variables, and S is the subset of variables excluding *i*. The function $f_{S\cup i}(x_{S\cup i})$ denotes the model output when variable *i* is included, while $f_S(x_S)$ represents the output when *i* is excluded. In general, tree-based machine learning algorithms like decision trees, random forest (RF), and XGBoost highlight the importance of input variables. In contrast, the

SHAP algorithm elucidates the interaction between independent and dependent variables (Xu et al., 2020). Recent applications of the SHAP algorithm include calculating the Shapley values for each variable to quantitatively assess their positive or negative correlations with air pollutants (Hou et al., 2022; Kang et al., 2023).

In this study, the RF model, one of the ensemble learning methods (Breiman, 2001) widely used in recent years, was employed to predict $PM_{2.5}$ concentrations. Recent studies have applied various machine learning algorithms (e.g., MLR, SVM, RF, and ANN) to predict air pollutant concentrations. Among these algorithms, the RF model has been demonstrated to have relatively high predictive performance for PM concentrations in South Korea (Lee et al., 2024b; Nam et al., 2022). The RF model in this study was trained using input variables that included the 59 target VOCs, criteria air pollutants (CAPs) such as SO_2, NO_2, O_3, and CO, and meteorological parameters including temperature, wind speed, relative humidity, atmospheric pressure, cloud cover, and ceiling height. The measured data for CAPs were obtained from 20 air quality monitoring stations (AQMSs) during the sampling period, accessed via the Air Korea website (https://www.airkorea.or.kr) (Fig. S1). Although most sampling sites corresponded with AQMS locations, discrepancies existed between the locations of AQMSs and AWSs, which did not perfectly match the sampling sites. For these cases, data for CAPs and meteorological parameters at the sampling sites were derived from their spatial distributions, interpolated using inverse distance weighting (IDW) in geographic information system software (ArcGIS 10.8.2, ESRI, USA). Finally, the contributions and interactions of individual VOCs to the predicted $PM_{2.5}$ levels were investigated using the SHAP algorithm with the RF model. The prediction model was implemented using the "treeshap" and "randomForest" packages in R software (version 4.3.1, R Core Team, Austria).

The prediction performance of the RF model was evaluated using several statistical indicators: correlation coefficient (R), root mean square error (RMSE), mean bias error (MBE), and mean absolute error (MAE). The dataset was split into training (70%) and verification (30%) sets. Prediction accuracy was then assessed through 50 iterations of random splits between these datasets. The comparison between the actual and predicted concentrations of $PM_{2.5}$ yielded values of $R = 0.78$, RMSE = 0.78 μg/m^3, MBE = 0.15 μg/m^3, and MAE = 0.67 μg/m^3, respectively. These results suggest that the RF model performs reliably in variable analysis for this study.

3. Results and discussion

3.1. Levels and spatial distributions of VOCs

The concentrations (mean ± standard deviation (SD)) of individual VOCs during the sampling period (July 28–August 4, 2021) are presented in Table S2. The highest mean concentration was observed for m, p-xylenes (5.5 ± 2.6 μg/m^3), followed by toluene (4.6 ± 2.5 μg/m^3), ethylbenzene (3.2 ± 1.5 μg/m^3), o-xylene (3.0 ± 1.4 μg/m^3), vinyl acetate (2.5 ± 2.1 μg/m^3), 1,2,4-trimethylbenzene (TMB) (2.4 ± 1.1 μg/m^3), styrene (1.1 ± 1.1 μg/m^3), methyl ethyl ketone (MEK) (0.9 ± 0.2 μg/m^3), and naphthalene (0.7 ± 0.3 μg/m^3). Toluene, ethylbenzene, and m,p,o-xylenes (TEX) collectively accounted for 56.9% of the total (Σ_{59}) VOCs. These compounds are well-known indicators of solvent use in activities such as painting, spraying, and coating, particularly under conditions favorable for evaporation during warm seasons (Gu et al., 2020; Li et al., 2020b). Similar to this study, seasonal (spring, summer, fall, and winter) monitoring studies previously conducted in Ulsan (Kim et al., 2019, 2023) showed that TEX contributed significantly (70.4 ± 9.7% and 43.6 ± 12.0%, respectively), likely due to substantial emissions from the industrial complexes. On the other hand, in this summer study, the mean concentration and fraction of benzene (0.5 μg/m^3 and 1.8%, respectively) were lower compared to its annual concentrations (2.21 and 2.24 μg/m^3) and fractions (8.2 and 4.0%) reported in earlier studies (Kim et al., 2019, 2023), as well as below the national air quality standard of 5.0 μg/m^3 (annual) in Korea (MOE, 2023). Therefore, higher contributions of TEX during the study period seem to be associated with the dominance of evaporation processes rather than combustion, which is generally more active in cold seasons (Bozkurt et al., 2018).

Fig. 2a represents the spatial distribution of Σ_{59} VOCs. Elevated concentrations were observed at most industrial sites (notably sites I1, I2, and I4) and several urban sites (sites U1, U2, U3, and U6) proximate to the industrial complexes involved in heavy chemical usage for automobile and ship manufacturing. Indeed, higher concentrations and emissions of TEX, which significantly contribute to Σ_{59} VOCs, were observed in both industrial complexes (Fig. S2). During the sampling period, southern winds predominated (Fig. 2b), suggesting that VOCs emitted from the industrial complexes along the East Sea could be transported inland toward urban areas (Kim et al., 2023). In addition, a wind rose diagram at the MO indicated that southeasterly winds were predominant during the sampling period, consistent with the summer 2021 pattern in this study area (Fig. S3). Therefore, exposure to VOCs in the urban area of Ulsan might be more pronounced during summer than in other seasons.

Several sites appear to be directly influenced by specific sources. For instance, a relatively high concentration of Σ_{59} VOCs (29.2 μg/m^3) was observed at site U11 (Fig. 2a), which corresponds to large toluene emissions reported in the PRTR for 2021 (Fig. S2a). Site I4, located in the petrochemical industrial complex, showed an exceptionally high concentration of styrene (5.6 μg/m^3), primarily emitted from the chemical industry and refineries (Wei et al., 2019), and vinyl acetate associated with emissions from the petrochemical sector (Zhao et al., 2004). The highest concentrations of toluene and MEK were measured at site U6, where construction of a new building was underway during the sampling period, reflecting emissions from building materials and consumer products (Du et al., 2014; WHO, 1992). Nearby the automobile and shipbuilding industrial complexes, sites I1, U1, and U3 showed elevated concentrations of 1,2,4-TMB, commonly linked to solvent use in automobile and ship manufacturing processes (Gu et al., 2020; Li et al., 2020b).

3.2. Evaluation of toluene/benzene ratios

Different diagnostic ratios have frequently been used for the source identification of VOCs. Among these, the toluene/benzene (T/B) ratio serves as a preliminary indicator to distinguish effects from vehicles versus solvents. For example, higher abundances of toluene generally result from solvent use and evaporation, while benzene is more indicative of fuel combustion (Ghosh et al., 2023; Sarmiento et al., 2023). A T/B ratio ranging from 1.5 to 4.3 suggests fuel combustion, while ratios outside of this range are classified as other sources (Hosseini et al., 2023). Particularly, a T/B ratio exceeding 10 is considered a strong indicator of solvent effects (Le et al., 2023).

Guided T/B ratios from previous studies are depicted alongside T/B ratios measured in the current and previous studies in South Korea (Fig. 3). A pronounced solvent effect was observed in industrial complexes in Daegu (Choi et al., 2009) and Siheung/Ansan (Kim et al., 2020) with notably higher mean ratios (11.3 and 21.3, respectively). On the other hand, the Namsan (Kim et al., 2012) and Sangdo (Na, 2006) tunnels in Seoul exhibited ratios of 2.1 and 2.2, respectively, falling within the range of 1.5–4.3, indicating fuel combustion effects (e.g., vehicular exhaust). The daily traffic volumes in 2020 for these four-lane tunnels were 33,026 and 69,640 vehicles, with lengths of 1270 m and 566 m, respectively.

The spatial distribution of mean T/B ratios during the sampling period is depicted in Fig. S4 to visually illustrate the effects of dominant sources. The mean T/B ratios observed in this study were 10.3 ± 6.7, suggesting that the solvent effect could be dominant at most sites. The mean ratios between urban (8.4 ± 3.7) and industrial (8.6 ± 2.2) sites were comparable, except for significantly high ratios at sites U6 (22.3) and U11 (32.4). While commercial solvents in urban areas may

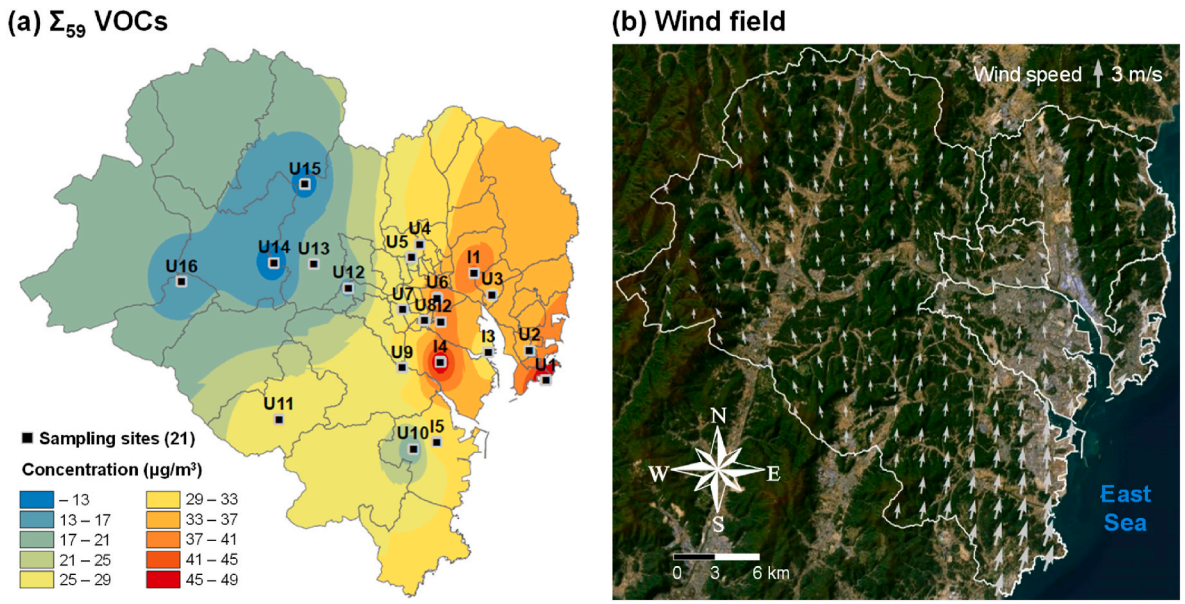

Fig. 2. Spatial distribution of (a) the concentration of total (Σ_{59}) VOCs and (b) the wind field during the sampling period. Details of the wind field are provided in Text S3.

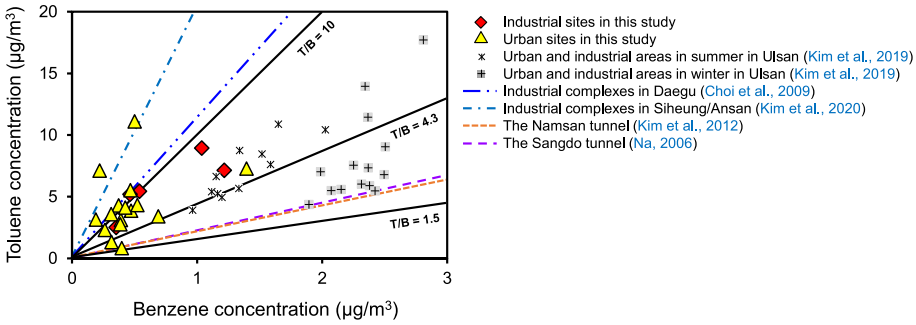

Fig. 3. Diagnostic ratios of toluene/benzene (T/B) at 5 industrial (red rhombuses) and 16 urban (yellow triangles) sites in this study, compared with findings from other studies conducted in urban and industrial areas in Ulsan (Kim et al., 2023), industrial complexes in Daegu (Choi et al., 2009) and Siheung/Ansan (Kim et al., 2020), and the Namsan (Kim et al., 2012) and Sangdo tunnels (Na, 2006).

contribute to higher ratios during warm atmospheric conditions, southeasterly winds during the sampling period are likely the main reason for elevated ratios at the urban sites. As mentioned previously, a new building was under construction next to site U6 during the sampling period. In a previous study, elevated concentrations of VOCs, especially toluene, were reported during the construction process (Du et al., 2014). The PRTR reported that the 4th and 6th highest emissions of toluene (255,566 and 9,424 kg/y, respectively) in 2021 were observed at two industrial facilities near site U11, out of a total of 206 industrial facilities in Ulsan.

The T/B ratios in our recent study conducted in Ulsan from 2019 to 2020 (Fig. 3) indicated distinct seasonal variations; fuel evaporation and combustion seem to be dominant in summer and winter, respectively (Kim et al., 2023). This is likely due to high temperatures in summer facilitating easy ventilation and evaporation of fuels and solvents, while combustion of fossil fuels tends to be more dominant during colder seasons. A similar seasonal variation of T/B ratios from 2014 to 2015 in Ulsan was reported (Kim et al., 2019). Therefore, this study area appears to be highly influenced by local fuel evaporation and solvent use during the sampling period. Additionally, three-day backward air trajectories suggest that local effects predominated over long-range atmospheric transport effects from China and North Korea, as shown in Fig. S5.

3.3. Human health risk assessment

Based on measured concentrations and a deterministic risk assessment approach, cancer and non-cancer risks were calculated for 13 carcinogens and 26 non-carcinogens, respectively (Fig. 4). The sampling period for this study (July 28–August 4, 2021) is insufficient to assess chronic risks from long-term exposure. However, significant amounts of VOCs are emitted continuously from the four industrial complexes in Ulsan, with little variation between seasons or years. Indeed, both the PRTR and the Clean Air Policy Support System (CAPSS, https://www.air.go.kr) have reported consistent emissions of toxic chemicals (mostly VOCs) and total VOCs from 2008 to 2021. Additionally, even though benzene levels were relatively low, the total concentration of BTEX was statistically comparable to those observed in our previous annual monitoring studies conducted in Ulsan during 2014–2015 (Kim et al., 2019) and 2019–2020 (Kim et al., 2023) (rank sum test, $p > 0.05$). A similar pattern was noted in our previous short-term (one week) study (Kim et al., 2024), which reported that short-term concentrations of benzene and m,p,o-xylenes were not significantly different from annual concentrations (rank sum test, $p > 0.05$). These findings suggest that industrial emissions of VOCs in Ulsan are relatively stable over time. Therefore, our short-term monitoring data may effectively represent long-term exposure.

As a result of individual cancer risk assessments, benzene (mean:

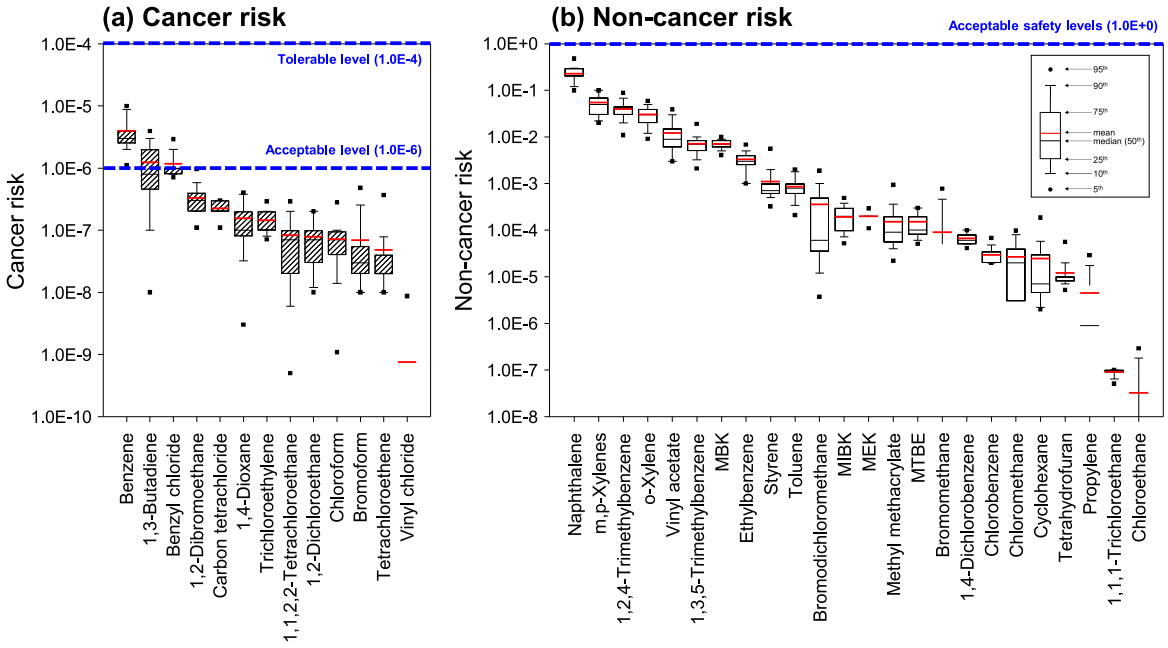

Fig. 4. Box plots of (a) cancer and (b) non-cancer risks for 13 carcinogens and 26 non-carcinogens, respectively. The blue lines represent the levels suggested by the US EPA, including acceptable, tolerable, and acceptable safety levels. Isopropyl alcohol and 1,1-dichloroethene, which were not detected in this study, are not included in the figure.

4.1E-6) was the most hazardous compound among the 13 carcinogens evaluated, followed by 1,3-butadiene (1.3E-6), benzyl chloride (1.2E-6), 1,2-dibromoethane (3.5E-7), and carbon tetrachloride (2.2E-7). The cancer risks associated with benzene, 1,3-butadiene, and benzyl chloride exceeded the acceptable level (1.0E-6) set by the US EPA (US EPA, 1991). However, all carcinogens, including benzene, presented cancer risks well below the more stringent tolerable level of 1.0E-4 (US EPA, 1991). Among the 26 non-carcinogens, naphthalene showed the highest mean HQ (2.3E-1), followed by m,p-xylenes (5.5E-2), 1,2,4-TMB (4.0E-2), o-xylene (3.0E-2), vinyl acetate (1.3E-2), and 1,3,5-TMB (7.4E-3). None of the individual non-cancer risks exceeded the acceptable safety level of 1.0 (US EPA, 1991). However, relatively higher HQs for naphthalene and m,p,o-xylenes may pose potential health risks, leading to adverse effects such as respiratory problems and neurological disorders (Mohammadi et al., 2020; Rostami et al., 2021). Previous studies in industrial areas have shown similar rankings for cancer and non-cancer risks, with benzene frequently reported as having much higher cancer risks, while 1,3-butadiene and carbon tetrachloride also displayed relatively high cancer risks (Baek et al., 2020; Scott et al., 2020). For non-carcinogens, the highest non-cancer risks were often found for naphthalene, with m,p-xylenes, o-xylene, 1,2,4-TMB, and 1,3,5-TMB tending to present higher risks than other species (Baek et al., 2020; Liu et al., 2023; Scott et al., 2020; Wang et al., 2023a). A relatively high non-cancer risk for vinyl acetate was also identified (Baek et al., 2020).

Additionally, cancer (Fig. S6) and non-cancer risk levels (Fig. S7) for individual VOCs were compared between industrial and urban sites. Overall, mean cancer and non-cancer risks of individual VOCs were higher at the industrial sites than at the urban sites, indicating a strong industrial impact in the study area. On the other hand, higher mean cancer risks at the urban sites than at the industrial sites were observed for several species, such as 1,3-butadiene (1.3E-6 at urban vs. 1.2E-6 at industrial), benzyl chloride (1.3E-6 vs. 1.1E-6), carbon tetrachloride (2.2E-7 vs. 2.1E-7), trichloroethylene (1.5E-7 vs. 1.4E-7), and tetrachloroethene (5.3E-8 vs. 3.2E-8) (Fig. S6). Despite these differences, the overall risk disparities between urban and industrial sites were minimal. These VOCs are emitted from urban sources such as vehicular exhausts and commercial products, yet industrial activities remain major contributors (ATSDR, 2005, 2019; US EPA, 1989, 2001, 2002). The urban sites exhibited higher mean non-cancer risks for MEK (1.9E-4 vs. 1.8E-4) and methyl methacrylate (1.8E-4 vs. 1.3E-4) (Fig. S7). As mentioned in Section 3.2, the construction of a new building at site U6 likely increased MEK concentrations (1.54 μg/m^3), which is typically emitted from building materials and consumer products (WHO, 1992). In contrast, a significantly higher concentration of methyl methacrylate (0.8 μg/m^3), mainly used in the plastics industry (US EPA, 1998), was observed at site U11 located near industrial facilities related to automobile components and plastic production. Overall, while urban emissions contributed to exposure, the predominant risk to human health arose from carcinogenic and non-carcinogenic VOCs emitted from the industrial complexes.

3.4. Secondary organic aerosol formation potential

3.4.1. Three different methods

Across all SOAFP calculation methods, toluene was the largest contributor, accounting for 29.3, 24.4, and 25.7% of the total SOAFPs, followed by m,p-xylenes (20.5, 21.9, and 18.9%), ethylbenzene (20.1, 18.8, and 15.9%), and o-xylene (17.8, 15.1, and 14.8%) (Fig. S8). Additionally, the combined contributions of 1,2,4-TMB and 1,3,5-TMB (7.3, 2.9, and 14.8%) were relatively high (Fig. S8). Benzene also ranked highly in total SOAFPs (2.5 and 7.3%) as calculated by the SOAP and SOA Yield methods, respectively (Figs. S8b and S8c). Notably, the SOAFP of styrene, only calculable by the SOAP method, was the fifth highest at 12.1% among the 18 VOCs examined (Fig. S8b). Previous studies (Chen et al., 2023; Zhang et al., 2023) have reported significant contributions from aromatic hydrocarbons, including BTEX, styrene, 1,2,4-TMB, 1,3,5-TMB, and 4-ethyltoluene to total SOAFPs. These aromatic hydrocarbons have stable chemical structures conducive to the condensation process and subsequent particle formation (Chen et al., 2023). In particular, styrene is highly reactive in terms of SOA formation (Zhan et al., 2021). Consequently, managing anthropogenic VOCs, especially aromatic compounds primarily emitted from industrial activities, is a priority in this study area.

The spatial distributions of total SOAFPs calculated by the three methods are depicted in Fig. 5. Overall, their spatial distributions are comparable across methods; however, the SOA Yield method showed higher SOAFPs than the other two methods, suggesting quantitative variations in SOAFP calculations. Despite this, the priority species and their spatial distributions remained similar. Notably, higher SOAFPs were observed near site U11 (influenced by direct sources of toluene) and around the petrochemical, automobile, and shipbuilding industrial complexes where elevated concentrations of Σ_{59} VOCs were found (Fig. 2a). Further analysis of the spatial distributions of SOAFPs (Fig. 5) alongside $PM_{2.5}$ data measured at the AQMSs during the sampling period (Fig. S9) revealed that areas near the petrochemical industrial complex consistently showed higher levels of both SOAFPs and $PM_{2.5}$. Relatively high concentrations were also observed at site U11 in both spatial distributions. On the other hand, the densely populated area around site U7 exhibited higher $PM_{2.5}$ concentrations, while the automobile and shipbuilding industrial complexes on the east of the study area (e.g., sites U1, U2, U3, and I1) showed elevated SOAFPs. Therefore, the petrochemical industrial complex may require prioritized management for SOA formation by VOCs, although the spatial distributions of SOAFPs (Fig. 5) and $PM_{2.5}$ (Fig. S9) were not perfectly aligned. The discrepancy between the spatial distributions of SOAFPs and $PM_{2.5}$ could be mainly due to differences in primary emissions and secondary formation. SOAs contributing to secondary $PM_{2.5}$ are generated by both anthropogenic and biogenic VOCs, whereas only a limited number of species were considered in this study. Furthermore, the simulation used for SOAFP calculation may not be fully adequate for this specific domestic study area. Additionally, this discrepancy could be partially attributed to variations in primary emission profiles for both $PM_{2.5}$ and VOCs. For instance, 2021 data from the CAPSS in Ulsan indicated that the highest $PM_{2.5}$ emissions originated from production processes (32% of total emissions), followed by non-road transport sources (26%), manufacturing industrial combustion (13%), fugitive dust (10%), waste disposal (6%), energy industrial combustion (5%), and biomass burning (4%). In contrast, VOC emissions were highest from production processes (59%), with the next highest emissions from solvent usage (23%), followed by waste disposal (10%) and energy transport and storage (5%) (https://www.air.go.kr).

The contributions of total SOAFPs to the measured $PM_{2.5}$ concentrations were compared between this study and previous studies (Table S4). The contributions differed among methods: FAC (mean: 8.4%, range: 3.1–15.5%), SOAP (10.1%, 3.8–18.0%), and SOA Yield (19.9%, 8.2–37.1%). These variations in SOAFPs across different methods have been frequently reported in prior studies (Han et al., 2018; Zhang et al., 2020). Different methods have varying parameters based on background environmental conditions (e.g., NO_X levels, temperature, oxidant concentration, and radiative flux) considered in smog chamber experiments and photochemical trajectory models (Zhang et al., 2017). Near industrial facilities, SOAFPs calculated by the FAC accounted for 2.4–75.6% (Han et al., 2018), 3.5% (Mozaffar et al., 2020), and 8.7–26.4% (Zhang et al., 2020) of $PM_{2.5}$. The SOAFPs by the SOA Yield were in ranges of 9.3–18.0% (Han et al., 2018) and 1.6–4.2% (Zhang et al., 2020) of $PM_{2.5}$. In urban areas, SOAFPs estimated by the SOAP and SOA Yield contributed 13.6–41.5% (Hui et al., 2019) and 9.2% (Han et al., 2017) to $PM_{2.5}$, respectively. Apart from these studies, another study estimated secondary organic carbon, which constitutes 3.8–17.7% of $PM_{2.5}$, based on measurements of organic and elemental carbon at urban sites (Feng et al., 2009). During a severe haze event, SOA contributed 30.0–77.0% to $PM_{2.5}$ in urban cities (Huang et al., 2014). Overall, the SOAFPs in this study are comparable to those in previous studies, although contributions to the corresponding $PM_{2.5}$ concentrations may vary depending on the study areas and target VOC species. In general, SOAFP tends to be underestimated due to the limited number of species considered and the inability to fully simulate the complex reactions of VOCs with OH radicals, NO_3, and O_3 in the atmosphere (Han et al., 2017, 2018; Zhang et al., 2020). Furthermore, this study did not include measurements of biogenic VOCs, which are known as important SOA precursors. Nonetheless, the findings of this study highlight that SOAFPs can contribute up to 37.1% to $PM_{2.5}$, implying a significant potential influence of anthropogenic VOCs on $PM_{2.5}$ levels in Ulsan.

3.4.2. *Application of XAI*

In this section, although the RF model was applied to the 59 target VOCs, detailed analysis was conducted on only 13 VOCs (1,2,4-TMB, 1,3,5-TMB, 4-ethyltoluene, benzene, cyclohexane, ethylbenzene, heptane, m,p-xylenes, MEK, naphthalene, o-xylene, styrene, and toluene), which were identified as significant contributors to total SOAFPs. Fig. 6 presents the summary plot of Shapley values for these VOCs. Styrene emerged as the most influential variable for the predicted $PM_{2.5}$ concentrations, followed by o-xylene, m,p-xylenes, and ethylbenzene. Although the SOAFP for styrene can only be calculated using the SOAP method, previous studies reported that styrene is a key contributor to SOA formation in industrial cities (Derwent et al., 2010; Wu and Xie, 2018). In addition, while the SOAFP estimates potential SOA concentrations based solely on VOC concentrations and the coefficients of each method, the Shapley value calculates the contribution of VOCs to $PM_{2.5}$ concentrations by considering sampling locations and the presence of different species. Although the results of SOAFP and the Shapley value may differ, the Shapley value allows for a more detailed investigation of specific VOCs associated with $PM_{2.5}$ concentrations under the pollution conditions in Ulsan. Therefore, correlations between styrene concentrations and Shapley values at the sampling sites were examined (Fig. S10). Elevated Shapley values were observed in the petrochemical and non-ferrous industrial complexes (e.g., sites I2, I3, I4, and I5) and some urban sites near the industrial complexes (e.g., sites U1, U6, U7,

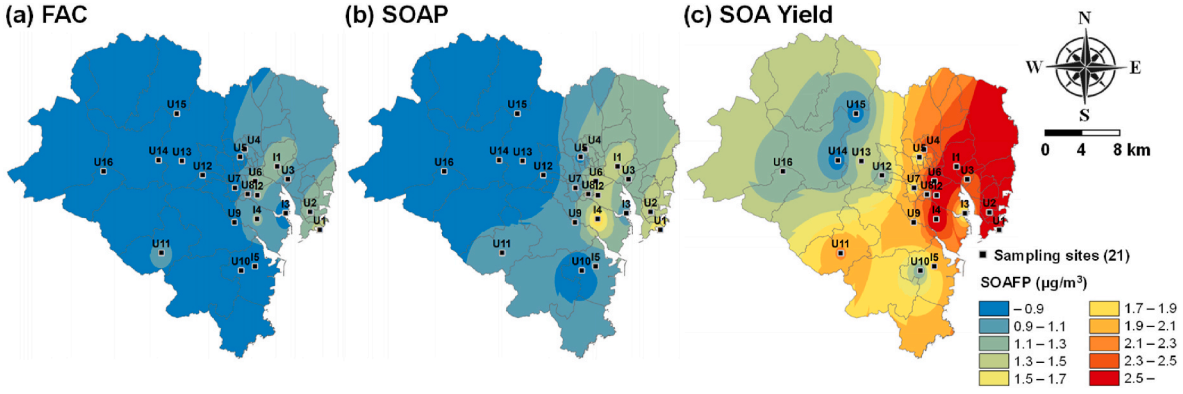

Fig. 5. Spatial distribution of secondary organic aerosol formation potentials (SOAFPs) calculated using (a) the fractional aerosol coefficient (FAC), (b) secondary organic aerosol potential (SOAP), and (c) secondary organic aerosol (SOA) Yield methods.

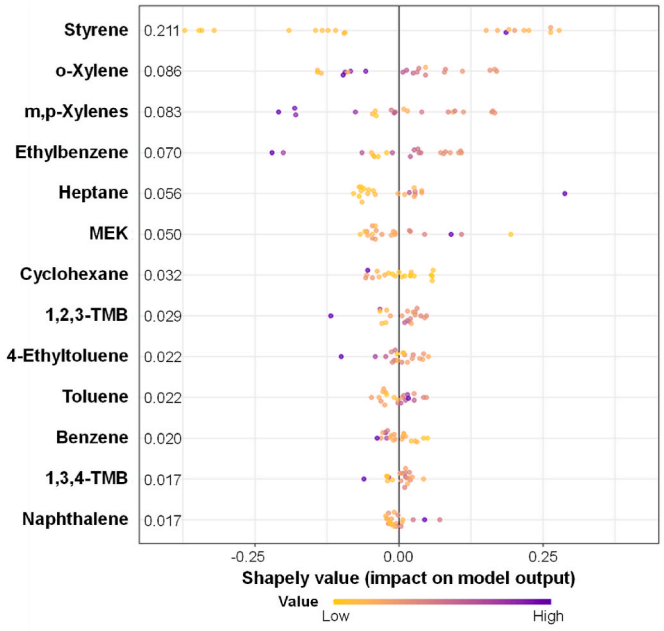

Fig. 6. Summary plot of Shapley values from the Shapley Additive Explanations (SHAP) algorithm for the 13 VOCs significantly contributing to total SOAFPs. The X-axis indicates the impact of each VOC on $PM_{2.5}$ prediction, with points colored to represent individual passive air samples and their respective feature values (levels of individual species). Numbers adjacent to the VOC names indicate their average absolute Shapley values.

U8, U9, and U11), where styrene concentrations exceeded 0.86 μg/m^3. This result implies that styrene emissions from these industrial complexes might be linked to increased $PM_{2.5}$ levels. In Ulsan, major sources of styrene include petroleum refinery storage tanks and rubber/resin factories (Fig. S11). Styrene emitted from industrial areas is known to degrade rapidly, producing phenoxy radicals that contribute significantly to SOA formation (Derwent et al., 2010). Therefore, it is anticipated that styrene emissions from the petrochemical complex play a crucial role in SOA formation in Ulsan. Additionally, the spatial distribution of Shapley values for styrene was compared with the distributions of $PM_{2.5}$ and styrene concentrations (Fig. S12). These spatial distributions align closely, particularly in the petrochemical industrial complex, indicating hot spots. Notably, the spatial distributions of $PM_{2.5}$ concentrations and Shapley values show a high degree of similarity. The results of the SHAP algorithm underscore the importance of monitoring styrene in addition to TEX, which were identified as primary contributors to $PM_{2.5}$ in this study.

3.5. Listing of priority VOCs

In this section, we present a list of priority VOCs selected from the 59 VOCs analyzed, based on their concentrations, risks, and SOAFPs. The prioritization includes (1) a ranking of the concentrations for all 59 VOCs, (2) rankings of risks for 13 carcinogens and 26 non-carcinogens, and (3) rankings of SOAFPs determined by the FAC, SOAP, and SOA Yield methods for 10, 18, and 10 VOCs, respectively. The top 10 VOCs from each category are detailed in Table 1. Additionally, this section explores the use of XAI to support VOC prioritization. It also examines the relative importance of these compounds and their implications for management strategies. As mentioned in the section on human health risk assessment, short-term monitoring of VOCs may raise concerns; however, given that VOC emissions from industrial complexes in Ulsan do not vary substantially between seasons or years, our study period is acceptable for proposing a priority list of VOCs based on their concentrations, risks, and SOAFPs.

Table 1
Top 10 VOCs ranked by their concentrations (μg/m^3), carcinogenic and non-carcinogenic risks, and SOAFPs (μg/m^3) estimated using the FAC, SOAP, and SOA Yield methods.

Concentration			Risk					Secondary organic aerosol formation potential								
			Carcinogen			Non-carcinogen		FAC			SOAP			SOA Yield		
1	m,p-Xylenes	5.51	1	Benzene	4.1E-6	1	Naphthalene	2.3E-1	1	Toluene	0.25	1	Toluene	0.25	1	Toluene	0.53
2	Toluene	4.63	2	1,3-Butadiene	1.3E-6	2	m,p-Xylenes	5.5E-2	2	m,p-Xylenes	0.18	2	m,p-Xylenes	0.23	2	m,p-Xylenes	0.39
3	Ethylbenzene	3.20	3	Benzyl chloride	1.2E-6	3	1,2,4-TMB	4.0E-2	3	Ethylbenzene	0.17	3	Ethylbenzene	0.19	3	Ethylbenzene	0.33
4	o-Xylene	3.01	4	1,2-Dibromoethane	3.5E-7	4	o-Xylene	3.0E-2	4	o-Xylene	0.15	4	o-Xylene	0.16	4	o-Xylene	0.30
5	Vinyl acetate	2.53	5	CCl_4[b]	2.2E-7	5	Vinyl acetate	1.3E-2	5	1,2,4-TMB	0.05	5	Styrene	0.12	5	1,2,4-TMB	0.25
6	1,2,4-TMB[a]	2.42	6	1,4-Dioxane	1.7E-7	6	1,3,5-TMB	7.4E-3	6	Naphthalene	0.03	6	1,2,4-TMB	0.03	6	Benzene	0.15
7	Styrene	1.08	7	Trichloroethylene	1.5E-7	7	MBK	7.3E-3	7	4-Ethyltoluene	0.02	7	Benzene	0.03	7	1,3,5-TMB	0.05
8	MEK	0.95	8	1,1,2,2-TECA[c]	8.6E-8	8	Ethylbenzene	3.2E-3	8	1,3,5-TMB	0.01	8	4-Ethyltoluene	0.02	8	Naphthalene	0.05
9	Naphthalene	0.69	9	1,2-Dichloroethane	8.2E-8	9	Styrene	1.1E-3	9	Heptane	0.00[d]	9	1,3,5-TMB	0.00[f]	9	Heptane	0.00[g]
10	4-Ethyltoluene	0.59	10	Chloroform	7.1E-8	10	Toluene	9.3E-4	10	Cyclohexane	0.00[e]	10	MEK	0.00[d]	10	Cyclohexane	0.00[g]

[a] Trimethylbenzene.
[b] Carbon tetrachloride.
[c] Tetrachloroethane.
[d] 0.0003.
[e] 0.0002.
[f] 0.003.
[g] 0.001.

Among all species, m,p-xylenes were consistently highly ranked across all three lists. The concentrations and SOAFPs of toluene and ethylbenzene were also high, but their associated risks were relatively low. o-Xylene, vinyl acetate, and 1,2,4-TMB had moderate rankings on the three lists. Vinyl acetate ranked fifth for both concentration and risk, but its SOAFP could not be calculated due to the lack of FAC, SOAP, and SOA Yield values. The concentrations of styrene, MEK, naphthalene, and 4-ethyltoluene were lower in the top 10 list, with styrene showing higher concentration and SOAFP than the other three, but a lower risk priority. On the other hand, naphthalene was the highest-ranked non-carcinogen, despite its lower SOAFP priority. MEK and 4-ethyltoluene had low SOAFP rankings and no associated risk data. Specifically, some compounds, like benzene, 1,3-butadiene, and benzyl chloride, while having relatively low concentration levels (13th, 25th, and 32nd, respectively, among 59 species), were highly ranked for risks, suggesting a high potential for adverse health impacts from long-term exposure even at lower concentrations. Benzene, in particular, requires careful management due to both its risk and potential for secondary formation. In addition, the risk and SOAFP of 1,3,5-TMB warrant attention despite its absence from the concentration list.

Overall, aromatic compounds, including m,p-xylenes, o-xylene, toluene, ethylbenzene, 1,2,4-TMB, 1,3,5-TMB, styrene, 4-ethyltoluene, benzyl chloride, and naphthalene, were frequently listed in Table 1. These compounds are predominantly emitted from anthropogenic sources, such as industrial processes and vehicles (Sahu et al., 2020). Given that Ulsan is the largest industrial city in South Korea, large amounts of aromatic compounds are emitted from Ulsan. Therefore, these compounds should be prioritized in VOC management efforts. Additionally, it is essential to customize management strategies, as the ranking of species on the individual lists varies due to factors such as toxicity, atmospheric reactivity, and emission sources.

4. Conclusion

Passive air sampling for 59 VOCs was conducted at 21 sites in Ulsan, a major industrial city in South Korea. TEX were the most abundant compounds among all monitored species, with high concentrations observed in the automobile and shipbuilding industrial complexes, where industrial solvents are heavily used for manufacturing processes. Southeasterly winds and warm conditions during the sampling period likely enhanced the effect of industrial emissions. Based on the concentration levels, risks, and SOAFPs of the 59 compounds, lists of the top 10 VOC species were compiled. Aromatic compounds were frequently found on all the lists. However, the ranking of species on individual lists varied depending on their concentration, toxicity, and secondary reactivity. In conclusion, a comprehensive prioritization of major VOC species should be considered when developing VOC management strategies in multi-industrial cities.

CRediT authorship contribution statement

Seong-Joon Kim: Writing – original draft, Resources, Formal analysis, Data curation. **Sang-Jin Lee:** Resources, Formal analysis, Data curation. **Youwei Hong:** Project administration. **Sung-Deuk Choi:** Writing – review & editing, Supervision, Project administration.

Declaration of competing interest

The authors declare that they have no known competing financial interests or personal relationships that could have appeared to influence the work reported in this paper.

Acknowledgments

This work was supported by a grant from the National Institute of Environmental Research (NIER), funded by the Ministry of Environment of the Republic of Korea (NIER-2022-04-02-038 and NIER-2021-03-03-007). In addition, this study was supported by the National Research Foundation of Korea (NRF-2020R1A6A1A03040570) and the Foreign Cooperation Project of Fujian Province (2020I0038). We acknowledge EACL members at UNIST for sampling.

Appendix A. Supplementary data

Supplementary data to this article can be found online at https://doi.org/10.1016/j.atmosenv.2024.120982.

Data availability

Data will be made available on request.

References

Ait-Helal, W., Borbon, A., Sauvage, S., de Gouw, J.A., Colomb, A., Gros, V., Freutel, F., Crippa, M., Afif, C., Baltensperger, U., Beekmann, M., Doussin, J.F., Durand-Jolibois, R., Fronval, I., Grand, N., Leonardis, T., Lopez, M., Michoud, V., Miet, K., Perrier, S., Prévôt, A.S.H., Schneider, J., Siour, G., Zapf, P., Locoge, N., 2014. Volatile and intermediate volatility organic compounds in suburban Paris: variability, origin, and importance for SOA formation. Atmos. Chem. Phys. 14, 10439–10464.

ATSDR, 2005. Toxicological Profile for Carbon Tetrachloride. Agency for Toxic Substances and Disease Registry. https://www.atsdr.cdc.gov/toxprofiles/tp30.pdf. (Accessed 22 February 2024).

ATSDR, 2019. Toxicological Profile for Tetrachloroethylene. Agency for Toxic Substances and Disease Registry. https://www.atsdr.cdc.gov/toxprofiles/tp18.pdf. (Accessed 23 February 2024).

Baek, K.-M., Kim, M.-J., Kim, J.-Y., Seo, Y.-K., Baek, S.-O., 2020. Characterization and health impact assessment of hazardous air pollutants in residential areas near a large iron-steel industrial complex in Korea. Atmos. Pollut. Res. 11, 1754–1766.

Bozkurt, Z., Üzmez, Ö.Ö., Döğeroğlu, T., Artun, G., Gaga, E.O., 2018. Atmospheric concentrations of SO_2, NO_2, ozone and VOCs in Düzce, Turkey using passive air samplers: sources, spatial and seasonal variations, and health risk estimation. Atmos. Pollut. Res. 9, 1146–1156.

Breiman, L., 2001. Random forests. Mach. Learn. 45, 5–32.

Chen, Z.W., Ting, Y.C., Huang, C.H., Ciou, Z.J., 2023. Sources-oriented contributions to ozone and secondary organic aerosol formation potential based on initial VOCs in an urban area of Eastern Asia. Sci. Total Environ. 892, 164392.

Choi, S.W., Park, S.W., Lee, C.S., Kim, H.J., Bae, S., Inyang, H.I., 2009. Patterns of VOC and BTEX concentration in ambient air around industrial sources in Daegu, Korea. J. Environ. Sci. Health A 44, 99–107.

Dehghani, M.H., Norouzian Baghani, A., Fazlzadeh, M., Ghaffari, H.R., 2019. Exposure and risk assessment of BTEX in indoor air of gyms in Tehran, Iran. Microchem. J. 150, 104135.

Derwent, R.G., Jenkin, M.E., Utembe, S.R., Shallcross, D.E., Murrells, T.P., Passant, N.R., 2010. Secondary organic aerosol formation from a large number of reactive man-made organic compounds. Sci. Total Environ. 408, 3374–3381.

Du, Z., Mo, J., Zhang, Y., Xu, Q., 2014. Benzene, toluene, and xylenes in newly renovated homes and associated health risk in Guangzhou, China. Build. Environ. 72, 75–81.

Duan, C., Liao, H., Wang, K., Ren, Y., 2023. The research hotspots and trends of volatile organic compound emissions from anthropogenic and natural sources: a systematic quantitative review. Environ. Res. 216, 114386.

Feng, Y., Chen, Y., Guo, H., Zhi, G., Xiong, S., Li, J., Sheng, G., Fu, J., 2009. Characteristics of organic and elemental carbon in $PM_{2.5}$ samples in Shanghai, China. Atmos. Res. 92, 434–442.

Ghosh, B., De, M., Rout, T.K., Padhy, P.K., 2023. Study on spatiotemporal distribution and health risk assessment of BTEX in urban ambient air of Kolkata and Howrah, West Bengal, India: evaluation of carcinogenic, non-carcinogenic and additional leukaemia cases. Atmos. Pollut. Res. 14, 101878.

Grosjean, D., 1989. Parameterization of the formation potential of secondary organic aerosols. Atmos. Environ. 23, 1733–1747.

Grosjean, D., 1992. Insitu organic aerosol formation during a smog episode: estimated production and chemical functionality. Atmos. Environ. 26A, 953–963.

Gu, S., Guenther, A., Faiola, C., 2021. Effects of anthropogenic and biogenic volatile organic compounds on Los Angeles air quality. Environ. Sci. Technol. 55, 12191–12201.

Gu, Y., Liu, B., Li, Y., Zhang, Y., Bi, X., Wu, J., Song, C., Dai, Q., Han, Y., Ren, G., Feng, Y., 2020. Multi-scale volatile organic compound (VOC) source apportionment in Tianjin, China, using a receptor model coupled with 1-hr resolution data. Environ. Pollut. 265, 115023.

Han, D., Gao, S., Fu, Q., Cheng, J., Chen, X., Xu, H., Liang, S., Zhou, Y., Ma, Y., 2018. Do volatile organic compounds (VOCs) emitted from petrochemical industries affect regional $PM_{2.5}$? Atmos. Res. 209, 123–130.

Han, D., Wang, Z., Cheng, J., Wang, Q., Chen, X., Wang, H., 2017. Volatile organic compounds (VOCs) during non-haze and haze days in Shanghai: characterization and secondary organic aerosol (SOA) formation. Environ. Sci. Pollut. Res. 24, 18619–18629.

Hosseini, S.A., Abtahi, M., Dobaradaran, S., Hassankhani, H., Koolivand, A., Saeedi, R., 2023. Assessment of health risk and burden of disease induced by exposure to benzene, toluene, ethylbenzene, and xylene in the outdoor air in Tehran, Iran. Environ. Sci. Pollut. Res. 30, 75989–76001.

Hou, L., Dai, Q., Song, C., Liu, B., Guo, F., Dai, T., Li, L., Liu, B., Bi, X., Zhang, Y., 2022. Revealing drivers of haze pollution by explainable machine learning. Environ. Sci. Technol. Lett. 9, 112–119.

Huang, R.J., Zhang, Y., Bozzetti, C., Ho, K.F., Cao, J.J., Han, Y., Daellenbach, K.R., Slowik, J.G., Platt, S.M., Canonaco, F., Zotter, P., Wolf, R., Pieber, S.M., Bruns, E.A., Crippa, M., Ciarelli, G., Piazzalunga, A., Schwikowski, M., Abbaszade, G., Schnelle-Kreis, J., Zimmermann, R., An, Z., Szidat, S., Baltensperger, U., El Haddad, I., Prevot, A.S., 2014. High secondary aerosol contribution to particulate pollution during haze events in China. Nature 514, 218–222.

Hui, L., Liu, X., Tan, Q., Feng, M., An, J., Qu, Y., Zhang, Y., Cheng, N., 2019. VOC characteristics, sources and contributions to SOA formation during haze events in Wuhan, Central China. Sci. Total Environ. 650, 2624–2639.

Kalbande, R., Yadav, R., Maji, S., Rathore, D.S., Beig, G., 2022. Characteristics of VOCs and their contribution to O_3 and SOA formation across seasons over a metropolitan region in India. Atmos. Pollut. Res. 13, 101515.

Kang, E., Park, S., Kim, M., Yoo, C., Im, J., Song, C.-K., 2023. Direct aerosol optical depth retrievals using MODIS reflectance data and machine learning over East Asia. Atmos. Environ. 309, 119951.

Kim, K.H., Anthwal, A., Park, C.G., Job, S.J., Chae, Y.Z., Park, J.A., Jung, J.H., Sohn, J.R., Oh, J.M., 2012. Monitoring of polyaromatic hydrocarbons and volatile organic compounds in two major traffic tunnels in Seoul, Korea. Environ. Technol. 33, 1963–1976.

Kim, M.J., Seo, Y.K., Kim, J.H., Baek, S.O., 2020. Impact of industrial activities on atmospheric volatile organic compounds in Sihwa-Banwol, the largest industrial area in South Korea. Environ. Sci. Pollut. Res. 27, 28912–28930.

Kim, S.-J., Kwon, H.-O., Lee, M.-I., Seo, Y., Choi, S.-D., 2019. Spatial and temporal variations of volatile organic compounds using passive air samplers in the multi-industrial city of Ulsan, Korea. Environ. Sci. Pollut. Res. 26, 5831–5841.

Kim, S.-J., Lee, H.-Y., Lee, S.-J., Choi, S.-D., 2023. Passive air sampling of VOCs, O_3, NO_2, and SO_2 in the large industrial city of Ulsan, South Korea: spatial-temporal variations, source identification, and ozone formation potential. Environ. Sci. Pollut. Res. 30, 125478–125491.

Kim, S.-J., Lee, S.-J., Kim, H., Hong, Y., Choi, S.-D., 2024. Contribution of individual sources of volatile organic compounds to their cancer and non-cancer risks in the multi-industrial city of Ulsan, South Korea. Air Qual. Atmos. Health. 17, 1937–1949.

Kim, S.-J., Lee, S.-J., Lee, H.-Y., Park, H.-J., Kim, C.-H., Lim, H.-J., Lee, S.-B., Kim, J.Y., Schlink, U., Choi, S.-D., 2021. Spatial-seasonal variations and source identification of volatile organic compounds using passive air samplers in the metropolitan city of Seoul, South Korea. Atmos. Environ. 246, 118136.

Kim, S.-J., Lee, S.-J., Lee, H.-Y., Son, J.-M., Lim, H.-B., Kim, H.-W., Shin, H.-J., Lee, J.-Y., Choi, S.-D., 2022. Characteristics of volatile organic compounds in the metropolitan city of Seoul, South Korea: diurnal variation, source identification, secondary formation of organic aerosol, and health risk. Sci. Total Environ. 838, 156344.

Kumar, A., Singh, D., Kumar, K., Singh, B.B., Jain, V.K., 2018. Distribution of VOCs in urban and rural atmospheres of subtropical India: temporal variation, source attribution, ratios, OFP and risk assessment. Sci. Total Environ. 613–614, 492–501.

Le, T.H., Lin, C., Nguyen, D.H., Cheruiyot, N.K., Yuan, C.S., Hung, C.H., 2023. Volatile organic compounds in ambient air of a major Asian port: spatiotemporal variation and source apportionment. Environ. Sci. Pollut. Res. 30, 28718–28729.

Lee, B.-K., Choi, S.-D., Shin, B., Kim, S.-J., Lee, S.-J., Kim, D.-G., Lee, G., Kang, H.-J., Kim, H.-S., Park, D.-Y., 2023. Sensitivity analysis of volatile organic compounds to $PM_{2.5}$ concentrations in a representative industrial city of Korea. Asian J. Atmos. Environ. 17, 1–12.

Lee, J., Lee, S.-J., Kim, S.-J., Kim, S.-H., Lee, G., Chang, L.-s., Choi, S.-D., 2024a. Pollution characteristics and secondary formation potential of volatile organic compounds in the multi-industrial city of Ulsan, Korea. Atmos. Environ. 319, 120313.

Lee, S.-J., Song, C.-K., Choi, S.-D., 2024b. Past and recent changes in the pollution characteristics of PM_{10} and SO_2 in the largest industrial city in South Korea. Atmos. Environ. 319, 120310.

Li, C., Li, Q., Tong, D., Wang, Q., Wu, M., Sun, B., Su, G., Tan, L., 2020a. Environmental impact and health risk assessment of volatile organic compound emissions during different seasons in Beijing. J. Environ. Sci. 93, 1–12.

Li, J., Deng, S., Li, G., Lu, Z., Song, H., Gao, J., Sun, Z., Xu, K., 2022. VOCs characteristics and their ozone and SOA formation potentials in autumn and winter at Weinan, China. Environ. Res. 203, 111821.

Li, Q., Su, G., Li, C., Liu, P., Zhao, X., Zhang, C., Sun, X., Mu, Y., Wu, M., Wang, Q., Sun, B., 2020b. An investigation into the role of VOCs in SOA and ozone production in Beijing. China. Sci. Total Environ. 720, 137536.

Liu, C., Xin, Y., Zhang, C., Liu, J., Liu, P., He, X., Mu, Y., 2023. Ambient volatile organic compounds in urban and industrial regions in Beijing: characteristics, source apportionment, secondary transformation, and health risk assessment. Sci. Total Environ. 855, 158873.

Lundberg, S.M., Lee, S.-I., 2017. A unified approach to interpreting model predictions. Proceedings of the 31st International Conference on Neural Information Processing Systems 30, 4768–4777.

MOE, 2023. Annual Report of Air Quality, 2022. Ministry of Environment of the Republic of Korea (in Korean). https://library.me.go.kr/#/search/detail/5907379. (Accessed 22 January 2024).

Mohammadi, A., Ghassoun, Y., Lowner, M.O., Behmanesh, M., Faraji, M., Nemati, S., Toolabi, A., Abdolahnejad, A., Panahi, H., Heydari, H., Miri, M., 2020. Spatial analysis and risk assessment of urban BTEX compounds in Urmia, Iran. Chemosphere 246, 125769.

Mozaffar, A., Zhang, Y.-L., Fan, M., Cao, F., Lin, Y.-C., 2020. Characteristics of summertime ambient VOCs and their contributions to O_3 and SOA formation in a suburban area of Nanjing, China. Atmos. Res. 240, 104923.

Na, K., 2006. Determination of VOC source signature of vehicle exhaust in a traffic tunnel. J. Environ. Manag. 81, 392–398.

Nam, S., Shin, M.Y., Han, J.Y., Moon, S.Y., Kim, J.Y., Tchah, H., Lee, H., 2022. Correlation between air pollution and prevalence of conjunctivitis in South Korea using analysis of public big data. Sci. Rep. 12, 10091.

Ng, N.L., Kroll, J.H., Chan, A.W.H., Chhabra, P.S., Flagan, R.C., Seinfeld, J.H., 2007. Secondary organic aerosol formation from m-xylene, toluene, and benzene. Atmos. Chem. Phys. 7, 3909–3922.

NIER, 2010. Research on Hazardous Air Pollutants (HAPs) in Ulsan Area. National Institute of Environmental Research of the Republic of Korea (in Korean). https://library.me.go.kr/#/search/detail/5254234. (Accessed 11 January 2024).

NIER, 2020. Monitoring of Hazardous Air Pollutants in the Urban Area (VI). National Institute of Environmental Research of the Republic of Korea (in Korean). https://library.me.go.kr/#/search/detail/5697551. (Accessed 11 January 2024).

NIER, 2021a. Monitoring of Hazardous Air Pollutants in the Industrial Area (IV). National Institute of Environmental Research of the Republic of Korea (in Korean). https://library.me.go.kr/#/search/detail/5882173. (Accessed 12 January 2024).

NIER, 2021b. Secondary Formation Potential of Biogenic and Anthropogenic VOCs in Ulsan (I). National Institute of Environmental Research of the Republic of Korea (in Korean). https://library.me.go.kr/#/search/detail/5865876. (Accessed 25 November 2023).

NIER, 2022a. The satellite integrated joint monitoring of air quality (SIJAQ) (I) - based on the ground and airborne observations. National Institute of Environmental Research of the Republic of Korea (in Korean). https://library.me.go.kr/#/search/detail/5906469. (Accessed 20 December 2023).

NIER, 2022b. The Satellite Integrated Joint Monitoring of Air Quality (SIJAQ) (II) - Based on the Ground and Airborne Observations. National Institute of Environmental Research of the Republic of Korea (in Korean). https://library.me.go.kr/#/search/detail/5907463. (Accessed 21 November 2023).

NIER, 2022c. Secondary Formation Potential of Biogenic and Anthropogenic VOCs in Ulsan (II). National Institute of Environmental Research of the Republic of Korea (in Korean). https://library.me.go.kr/#/search/detail/5876681. (Accessed 26 November 2023).

Pandis, S.N., Harley, R.A., Cass, C.R., Seinfeld, J.H., 1992. Secondary organic aerosol formation and transport. Atmos. Environ. 26A, 2269–2282.

Rostami, R., Fazlzadeh, M., Babaei-Pouya, A., Abazari, M., Rastgho, L., Ghasemi, R., Saranjam, B., 2021. Exposure to BTEX concentration and the related health risk assessment in printing and copying centers. Environ. Sci. Pollut. Res. 28, 31195–31206.

Sahu, L.K., Yadav, R., Tripathi, N., 2020. Aromatic compounds in a semi-urban site of western India: seasonal variability and emission ratios. Atmos. Res. 246, 105114.

Sarmiento, H., Potgieter-Vermaak, S., Borillo, G.C., Godoi, A.F.L., Reis, R.A., Yamamoto, C.I., Pauliquevis, T., Polezer, G., Godoi, R.H.M., 2023. BTEX profile and health risk at the largest bulk port in Latin America, Paranagua Port. Environ. Sci. Pollut. Res. 30, 63084–63095.

Scott, P.S., Andrew, J.P., Bundy, B.A., Grimm, B.K., Hamann, M.A., Ketcherside, D.T., Li, J., Manangquil, M.Y., Nunez, L.A., Pittman, D.L., Rivero-Zevallos, A., Uhlorn, R., Johnston, N.A.C., 2020. Observations of volatile organic and sulfur compounds in ambient air and health risk assessment near a paper mill in rural Idaho, U.S.A. Atmos. Pollut. Res. 11, 1870–1881.

Stirnberg, R., Cermak, J., Kotthaus, S., Haeffelin, M., Andersen, H., Fuchs, J., Kim, M., Petit, J.-E., Favez, O., 2021. Meteorology-driven variability of air pollution (PM_1) revealed with explainable machine learning. Atmos. Chem. Phys. 21, 3919–3948.

US EPA, 1989. Integrated Risk Information System (IRIS) Chemical Assessment Summary: Benzyl Chloride. United States Environmental Protection Agency. https://iris.epa.gov/static/pdfs/0393_summary.pdf. (Accessed 24 February 2024).

US EPA, 1991. Risk Assessment Guidance for Superfund: Volume 1-Human Health Evaluation Manual (Part B, Development of Risk-Based Preliminary Remediation Goals). United States Environmental Protection Agency. https://semspub.epa.gov/work/HQ/192.pdf. (Accessed 19 January 2024).

US EPA, 1998. Toxicological Review of Methyl Methacrylate. United States Environmental Protection Agency. https://iris.epa.gov/static/pdfs/1000tr.pdf. (Accessed 23 February 2024).

US EPA, 2001. Sources, Emission and Exposure For Trichloroethylene (TCE) and Related Chemicals. https://ofmpub.epa.gov/eims/eimscomm.getfile?p_download_id=4824. (Accessed 23 February 2024).

US EPA, 2002. Health Assessment of 1,3-Butadiene. https://cfpub.epa.gov/ncea/iris/iris_documents/documents/supdocs/butasup.pdf. (Accessed 24 February 2024).

US EPA, 2009. Risk Assessment Guidance for Superfund Volume I: Human Health Evaluation Manual (Part F, Supplemental Guidance for Inhalation Risk Assessment). United States Environmental Protection Agency. https://semspub.epa.gov/work/HQ/140530.pdf. (Accessed 25 February 2024).

Wang, H., Hao, R., Xie, X., Li, G., Wang, X., Wu, W., Zhao, H., Zhang, Z., Fang, L., Hao, Z., 2023a. Emission characteristics, risk assessment, and scale effective control of VOCs from automobile repair industry in Beijing. Sci. Total Environ. 860, 160115.

Wang, Y., Cui, Y., He, Q., Fan, J., Li, Y., Liu, K., Guo, L., Wang, X., 2023b. Significant impact of VOCs emission from coking and coal/biomass combustion on O_3 and SOA formation in Taiyuan. China. Atmos. Pollut. Res. 14, 101671.

Wei, W., Ren, Y., Yang, G., Cheng, S., Han, L., 2019. Characteristics and source apportionment of atmospheric volatile organic compounds in Beijing, China. Environ. Monit. Assess. 191, 762.

WHO, 1992. Environmental Health Criteria 143 Methyl Ethyl Ketone. World Health Organization. https://www.inchem.org/documents/ehc/ehc/ehc143.htm. (Accessed 17 January 2024).

Wu, C.F., Liu, L.J., Cullen, A., Westberg, H., Williamson, J., 2011. Spatial-temporal and cancer risk assessment of selected hazardous air pollutants in Seattle. Environ. Int. 37, 11–17.

Wu, R., Xie, S., 2018. Spatial distribution of secondary organic aerosol formation potential in China derived from speciated anthropogenic volatile organic compound emissions. Environ. Sci. Technol. 52, 8146–8156.

Xiong, Y., Zhou, J., Xing, Z., Du, K., 2020. Optimization of a volatile organic compound control strategy in an oil industry center in Canada by evaluating ozone and secondary organic aerosol formation potential. Environ. Res. 191, 110217.

Xu, J., Wang, A., Schmidt, N., Adams, M., Hatzopoulou, M., 2020. A gradient boost approach for predicting near-road ultrafine particle concentrations using detailed traffic characterization. Environ. Pollut. 265, 114777.

Zhan, J., Feng, Z., Liu, P., He, X., He, Z., Chen, T., Wang, Y., He, H., Mu, Y., Liu, Y., 2021. Ozone and SOA formation potential based on photochemical loss of VOCs during the Beijing summer. Environ. Pollut. 285, 117444.

Zhang, H., Chen, C., Yan, W., Wu, N., Bo, Y., Zhang, Q., He, K., 2021. Characteristics and sources of non-methane VOCs and their roles in SOA formation during autumn in a central Chinese city. Sci. Total Environ. 782, 146802.

Zhang, X., Gao, S., Fu, Q., Han, D., Chen, X., Fu, S., Huang, X., Cheng, J., 2020. Impact of VOCs emission from iron and steel industry on regional O_3 and $PM_{2.5}$ pollution. Environ. Sci. Pollut. Res. 27, 28853–28866.

Zhang, Z., Sun, Y., Li, J., 2023. Characteristics and sources of VOCs in a coastal city in eastern China and the implications in secondary organic aerosol and O_3 formation. Sci. Total Environ. 887, 164117.

Zhang, Z., Wang, H., Chen, D., Li, Q., Thai, P., Gong, D., Li, Y., Zhang, C., Gu, Y., Zhou, L., Morawska, L., Wang, B., 2017. Emission characteristics of volatile organic compounds and their secondary organic aerosol formation potentials from a petroleum refinery in Pearl River Delta. China. Sci. Total Environ. 584–585, 1162–1174.

Zhao, W., Hopke, P.K., Karl, T., 2004. Source identification of volatile organic compounds in Houston, Texas. Environ. Sci. Technol. 38, 1338–1347.